Magnetic Resonance in Medicine 47:447–454 (2002)
DOI 10.1002/mrm.10104

In Vivo GABA Editing Using a Novel Doubly Selective Multiple Quantum Filter

Jun Shen,[1,2*] Douglas L. Rothman,[3] and Peter Brown[3]

A novel multiple quantum filtering method is proposed that uses a doubly selective pulse termed Delays Alternating with Nutations for Tailored Excitation (DANTE) for multiple quantum preparation. This method selectively prepares GABA-3 and GABA-4 into a multiple quantum state and suppresses all other resonances at 3.0 ppm in each single scan. Phantom tests demonstrated excellent GABA signal retention and complete suppression of overlapping metabolites. It is shown using numerical simulations that overlapping macromolecules are suppressed because the frequency of the first upfield 2π rotation of the doubly selective DANTE pulse coincides with that of the macromolecules at 1.72 ppm. Excellent suppression of overlapping macromolecules was demonstrated in vivo. Using this method the concentration of GABA in the occipital lobe of healthy volunteers was measured to be 1.21 ± 0.28 μmol/mL (mean ± SD, N = 9). Magn Reson Med 47:447–454, 2002.

Key words: GABA; multiple quantum; DANTE pulse; quantitation; macromolecules

GABA (4-aminobutyric acid) is the major inhibitory neurotransmitter in the mammalian brain (1). Alterations in GABAergic function are associated with a variety of neurological and psychiatric disorders (2–7). The accurate determination of GABA concentration in the brain is important for the study of GABA's role in normal and pathological brain functions. However, noninvasive in vivo measurement of GABA is fraught with difficulties due to its low concentration and the presence of overlapping resonances. Due to the significant spectral overlap at GABA-2 (2.3 ppm) and GABA-3 (1.9 ppm) resonances, GABA-4 (3.0 ppm) has been the primary target for the measurement of GABA using in vivo magnetic resonance spectroscopy (MRS). Around 3.0 ppm, where GABA-4 resonates, the methyl group of creatine dominates. Fortunately, the methyl group of creatine is not subject to the effects of J-coupling. This allows it to be suppressed or separated using a variety of spectroscopic techniques, such as J-editing (8–11), 2D J-resolved spectroscopy (12), longitudinal scalar order difference editing (13), and multiple quantum filtering (14,15). Of these methods, only the multiple quantum filtering techniques are capable of completely suppressing the dominant overlapping creatine signal, even under the presence of potential subject movement and significant inhomogeneity in the amplitude of static and radiofrequency (RF) fields (15).

Of equal importance, but not addressed by many GABA measurement methods, is the suppression of overlapping mobile macromolecule resonances at 3.0 ppm, which couple with the macromolecule resonances at 1.72 ppm. These macromolecule resonances have a sufficiently long T_2 to contribute substantial intensity at 3.0 ppm at the echo time (TE) used for GABA editing. In the two-step J-editing methods (8–10,16), macromolecules can be accounted for by placing the editing pulse on the GABA-3 resonance at 1.91 ppm, and in a subsequent experiment on the macromolecules at 1.72 ppm. Alternatively, the editing pulse may be alternated between 1.91 ppm and symmetrically about the macromolecules at 1.72 ppm (16). In comparison, the GABA signal measured by spectrally non- or semiselective methods could contain a significant amount of coedited macromolecules. There is also in vivo evidence of a possibly significant presence of glutathione in the human cortex (17,18). The cysteinyl CH_2 group of glutathione resonates at 2.87–2.94 ppm. Since the cysteinyl methylene protons are coupled to the α-CH proton at 4.56 ppm, their suppression also depends on the spectral selectivity of the GABA measurement methods used, regardless of the mechanism of creatine suppression.

In this work we present a novel doubly selective multiple quantum filtering technique for in vivo GABA measurement at 2.1 T. This method selectively prepares GABA-3 and GABA-4 into a multiple quantum state while suppressing overlapping resonances such creatine, macromolecules, and glutathione in each single scan. At the low field strength of 2.1 T, excellent suppression of the overlapping resonances of creatine and glutathione was achieved, with a dramatic improvement in macromolecule suppression. This method is illustrated in the following using numerical simulations, phantom experiments, and in vivo GABA measurements in the human brain.

METHODS

Numerical simulations were performed on a SPARC-Station 20 computer using an in-house C routine. For each Delays Alternating with Nutations for Tailored Excitation (DANTE) (19–21) pulse segment or free-precession interval, matrix multiplication based on Bloch equations without the relaxation terms was performed to calculate the sequential rotation of the magnetization as a function of frequency offset. The off-resonance effect during RF rotations was taken into account in the simulation.

All experiments were performed on a 2.1 T whole-body spectrometer (Bruker Medical Instruments, Billerica, MA)

[1]Center for Advanced Brain Imaging, Nathan S. Kline Institute for Psychiatric Research, Orangeburg, New York.

[2]Department of Radiology, New York University School of Medicine, New York, New York.

[3]Department of Diagnostic Radiology, Yale University School of Medicine, New Haven, Connecticut.

Grant sponsor: NIH; Grant numbers: R01 RR 15106; NS 37527; Grant sponsor: NARSAD.

*Correspondence to: Jun Shen, Ph.D., Center for Advanced Brain Imaging, Nathan S. Kline Institute for Psychiatric Research, 140 Old Orangeburg Rd., Orangeburg, NY 10962. E-mail: shen@nki.rfmh.org

Received 3 May 2001; revised 4 September 2001; accepted 14 November 2001.

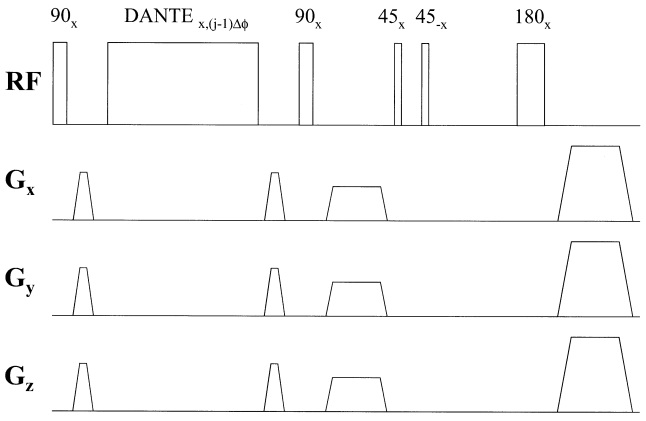

FIG. 1. The proposed pulse sequence for doubly selective multiple quantum detection of GABA-4. All RF pulses are applied along the *x*-axis except the even-numbered RF components in the doubly selective DANTE pulse, which have a linear phase increment of 90° ($\Delta\phi$ = 90°, j = 1, . . ., n). The theoretical interpulse delay between the odd- or the even-numbered pulses is $\Delta\phi/|\upsilon_{GABA\text{-}4} - \upsilon_{GABA\text{-}3}|$. The doubly selective DANTE pulse selectively refocuses the chemical shift evolution of GABA-3 and GABA-4 spins without inhibiting the evolution of their mutual J-coupling terms. The second 90° pulse along the *x*-axis converts the antiphase coherences into GABA-3/-4 double quantum coherence. The multiple quantum preparation is preceded by CHESS pulses for water suppression, then an outer-volume suppression (OVS) scheme along –*x*, *x*, –*y*, –*z*, and *z*, as well as spatial localization pulses using 3D ISIS. The CHESS, OVS, and ISIS schemes were not drawn for clarity.

with an actively shielded body gradient system. The maximum usable gradient strength on all three axes is 1.4 × 10^{-2} T/m with a rise time of 1.1 ms. A volume coil driven in linear mode was used for RF transmission with an 8-cm surface coil for detection. The two coils were actively decoupled by pin-diode switches controlled by the pulse sequences. Human subjects were placed supine on a patient bed with the head positioned so that the occipital lobe was directly above the center of the surface receiver coil. A multislice transverse and sagittal gradient-echo imaging sequence was used for subject or phantom positioning and for selection of a 3 cm × 3 cm × 3 cm voxel in the occipital lobe for localized GABA measurement. An automatic shimming method was used for minimization of the first- and second-order static field inhomogeneity within the selected voxel (22,23). RF pulse power for a nonselective 180° pulse was calibrated in vivo by generating a null signal within the selected voxel using a 2D stimulated echo sequence that selected a 1 cm × 1 cm *y* column through the center of the selected voxel. All nonselective RF pulses were set at the same power level. The RF power settings for selective RF pulses were calculated based on the predetermined RF power relationships between the nonselective 180° pulse and the selective pulses. The creatine resonance frequency at 3.0 ppm was measured using a STimulated Echo Acquisition Mode (STEAM) sequence (three 90° five-lobe sinc pulses, TE = 68 ms) to select the same 3 cm × 3 cm × 3 cm volume as the GABA sequence.

The GABA sequence used in this study is shown in Fig. 1. Initially, a CHEmical-Shift-Selective (CHESS) sequence consisting of three 90° CHESS Gaussian pulses, each followed by a gradient crusher, was used for water suppression. The outer volume suppression (OVS) scheme consists of five 90° spatially-selective five-lobe sinc pulses and crusher gradients suppressing five 3.6-cm-thick slabs along –*x*, *x*, –*y*, –*z*, and *z*. The 3 cm × 3 cm × 3 cm volume for GABA measurement was localized by a 3D Image-Selected In vivo Spectroscopy (ISIS) method using three hyperbolic secant pulses (μ = 4, 1% truncation). The multiple quantum preparation sequence consists of a nonselective 90° pulse on *x*, a nominal delay of 1/8J, a doubly selective DANTE pulse with π rotations at 3.0 pm and 1.91 ppm, a second nominal delay of 1/8J, and a second nonselective 90° pulse on *x*. The doubly selective DANTE pulse consists of 31 pieces of RF segments with an interpulse delay of 1248 μs. The phase of the odd-numbered RF segments was set to zero. For easy implementation the phase increments for the even-numbered RF segments were set to 90°. Resonances not refocused by the doubly selective DANTE pulse are dephased by gradient crushers. Immediately after the multiple quantum preparation, the double quantum coherence is encoded by 4-ms gradient pulses along all three axes. The double quantum coherence is then converted into an anti-phase GABA-4 single quantum coherence by a semiselective pulse with 90° excitation on GABA-3 and 0° excitation on GABA-4. In the last step, the GABA-4 signal is rephased over a period of 1/4J using a nonselective 180° refocusing pulse. The double quantum filtering gradients are three 8-ms gradient pulses of the same strength as the double quantum encoding gradients.

RESULTS

Numerical Simulation

Figure 2 shows the frequency response of the doubly selective DANTE pulse acting on equilibrium magnetization

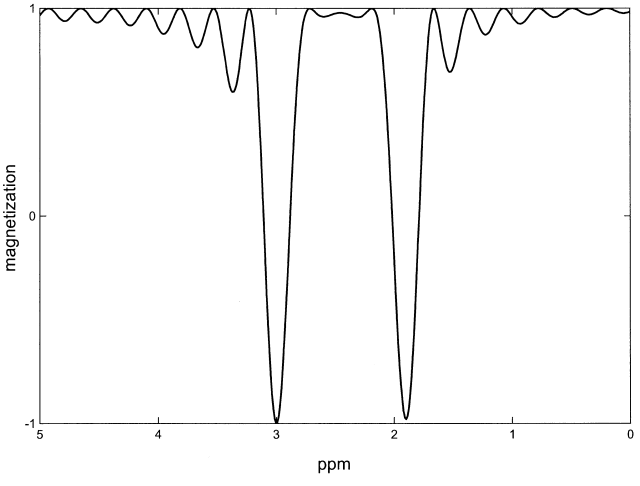

FIG. 2. Bloch simulation of the frequency response of the doubly selective DANTE pulse acting on equilibrium magnetization over the 0–5 ppm region. The π rotations are located at the GABA-3 and GABA-4 frequencies. The first upfield 2π null lies approximately at the frequency offset of the macromolecules, which are coupled to the overlapping macromolecules at 3.0 ppm.

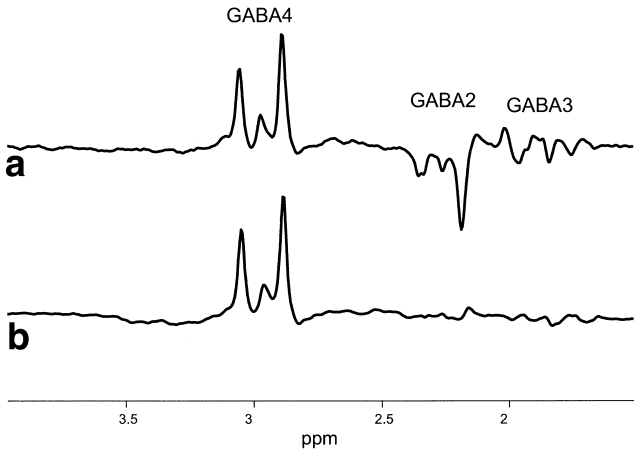

FIG. 3. **a:** Spectrum acquired using the nonselective multiple quantum preparation method from a spherical phantom containing GABA and creatine in a 1:8 molar ratio. **b:** Spectrum acquired using the doubly selective DANTE multiple quantum preparation method on the same phantom sample. The residual central line in the GABA-4 peak is due to the strong coupling effect between GABA-3 and GABA-4. A 106% retention of the two outer resonance lines was obtained using the doubly selective multiple quantum preparation method with respect to the nonselective preparation method.

over the 0–5 ppm region at 2.1 T. The other set of sidebands, which lies in the 0–10 ppm range, is located at 6.3 and 7.4 ppm, respectively. Clearly, ca. 100% inversion was obtained at the resonance frequencies of both GABA-3 and GABA-4. At each resonance frequency, due to the close proximity of the two frequencies (24), deviation from the symmetrical response of a singly selective DANTE pulse is prominent, especially in the region sandwiched by the two inversion bands. The first upfield 2π null of the doubly selective DANTE pulse lies at 1.70 ppm, very close to the frequency offset of the macromolecules, which are coupled to the overlapping macromolecule resonance at 3.0 ppm (25). The quaternion elements (26,27) of the overall propagator of the refocusing doubly selective DANTE pulse as a function of frequency offset were also calculated numerically. The π rotations (quaternion element $l_{xx}\sin(\beta/2) = 1$) at GABA-4 and GABA-3, and the approximately 2π rotation (quaternion element $l_{xx}\sin(\beta/2) \approx 0$) at 1.72 ppm were confirmed (data not shown).

Creatine Suppression and GABA Retention

Excellent creatine suppression was achieved using both nonselective and doubly selective multiple quantum preparation methods as demonstrated in Fig. 3. The spectrum shown in Fig. 3a was acquired using the pulse sequence described in Methods, except that the doubly selective DANTE pulse was replaced by a nonselective 180° rectangular pulse with a multiple quantum preparation delay of 34 ms. A spherical phantom containing GABA and creatine in a 1:8 molar ratio (buffered to pH = 7.0 using KH_2PO_4 and K_2HPO_4) was used. The spectrum shown in Fig. 3b was acquired using the doubly selective DANTE multiple quantum preparation method from the same phantom. Using a phantom sample containing a solution of only creatine, the creatine suppression ratio was estimated to be ca. 1500:1 for the doubly selective DANTE method. The efficiency of the multiple quantum preparation using the refocusing doubly selective DANTE pulse was assessed by comparing its retention of GABA-4 signal intensity with that of the nonselective preparation. Based on the intensities of the outer resonance lines shown in Fig. 3, the doubly selective DANTE method implemented on the 2.1 T spectrometer retains 106% of the GABA-4 signal with respect to the nonselective multiple quantum preparation method.

Glutathione Suppression

To demonstrate suppression of other possibly interfering metabolites that have coupled spins around 3.0 ppm, glutathione (whose cysteinyl methylene group resonates at 2.87–2.94 ppm) was used as an example. Figure 4a shows a glutathione spectrum obtained from a cylindrical phantom sample (11.5 cm in diameter) containing only glutathione and inorganic phosphates (pH = 7.5) using the STEAM sequence described in Methods. Then the doubly selective multiple quantum filtering sequence was applied, which effectively suppressed the glutathione signal (see Fig. 4b). When GABA was added to the same phantom sample ([glutathione] : [GABA] = 2:1, pH = 7.5) the doubly selective multiple quantum filtering sequence with parameters identical to those used in Fig. 4b revealed the GABA-4 signal as shown in Fig. 4c. From the 2:1 molar

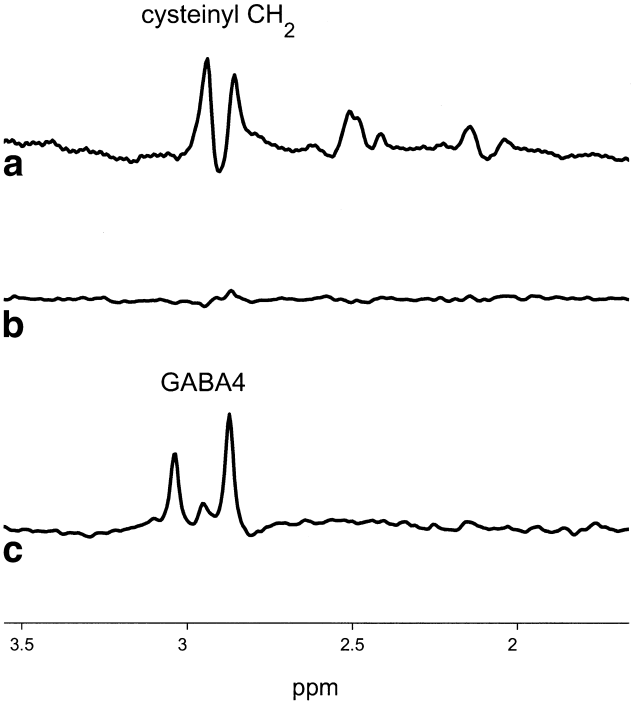

FIG. 4. **a:** STEAM spectrum of glutathione solution in a cylindrical bottle phantom at TE = 68 ms. **b:** The pulse sequence was switched to the doubly selective multiple quantum filtering sequence, which effectively suppressed the cysteinyl methylene proton signal. **c:** The same doubly selective multiple quantum filtering sequence was applied to the phantom sample after addition of GABA ([glutathione] : [GABA] = 2:1).

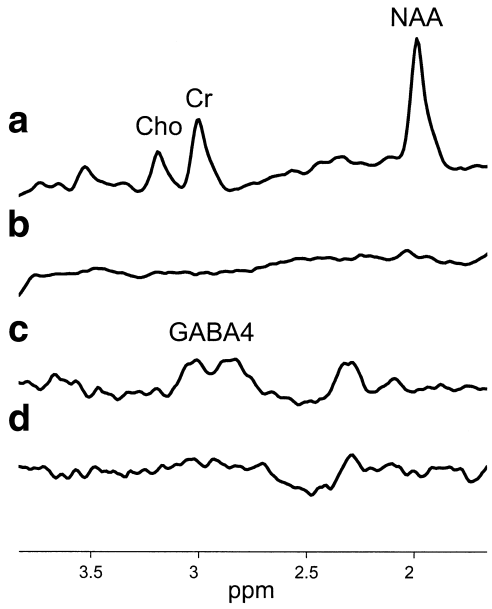

FIG. 5. **a:** In vivo STEAM spectrum from a 3 × 3 × 3 cm^3 volume in the occipital lobe of a healthy subject. Acquisition parameters were: TR = 3.3 s, TE = 68 ms, and NS = 32. **b:** A nonselective hyperbolic secant inversion pulse and 0.86 s IR delay was added to the STEAM pulse sequence to obtain a metabolite null. The same acquisition and processing parameters as in **a** were applied here. **c:** In vivo GABA spectrum from the same 3 × 3 × 3 cm^3 volume in the occipital lobe. Acquisition parameters were: TR = 3.3 s, nominal TE = 68 ms, and NS = 256. **d:** The same IR scheme was applied to the GABA sequence. The same acquisition and processing parameters as in **c** were applied here. The vertical scales used in **a–d** are the same.

ratio of glutathione to GABA the glutathione suppression ratio was determined to be 51:1.

Macromolecule Suppression

To estimate the macromolecule contribution to the signal at 3.0 ppm acquired using the doubly selective multiple quantum filtering method, in vivo spectra were acquired in which metabolite resonances were nulled by an inversion-recovery (IR) pulse (11,25) from a 3 × 3 × 3 cm^3 volume in the occipital lobe of healthy adult subjects. Figure 5a shows a nonedited in vivo spectrum using the STEAM sequence described in the Methods section. The TR was set to 3.3 s. Thirty-two scans were acquired for signal averaging. Then a nonselective 10-ms hyperbolic secant inversion pulse (μ = 4, 1% truncation) was applied with an IR delay of 0.86 s prior to the first 90° pulse of the STEAM sequence. This resulted in a "metabolite null," as shown in Fig. 5b, due to similar T_1 values for all metabolites at 2.1 T (25). Note that at the relatively long TE used here (64 ms, $\approx 1/(2^3 J_{HH})$) the intensities of the coupled spins, such as glutamate, glutamine, and macromolecules, are dramatically reduced in Fig. 5a and b due to the combined effects of T_2 relaxation and/or J evolution into antiphase magnetization. The typical spectral feature at the metabolite null seen in a short-TE spectrum is largely absent in Fig. 5b, as expected. Figure 5c shows the in vivo GABA spectrum acquired using the doubly selective DANTE multiple quantum pulse sequence shown in Fig. 1. As in the STEAM method, TR was set to 3.3 s. Two hundred fifty-six scans were acquired for signal averaging. GABA-4 and the residual overlapping macromolecules were seen at 3.0 ppm (Fig. 5c). When the same IR scheme is used in the GABA sequence, the remaining signal at 3.0 ppm (Fig. 5d) should be predominantly macromolecules because the T_1 of macromolecules at 2.1 T has been previously determined in vivo to be 0.25 s with 3D ISIS localization (25). Thus, macromolecules are at 94% of their full intensity with the IR delay of 0.86 s used here. Using the following equation,

$$f_{macromolecues} = \frac{S_{metabolite-null}}{0.94 S_{no\ metabolite-null}} \quad [1]$$

the contribution of macromolecules to GABA-4 ($f_{macromolecules}$) can be estimated from the signal intensities at 3.0 ppm with ($S_{metabolite\text{-}null}$) and without ($S_{no\ metabolite\text{-}null}$) the metabolite null.

At 2.1 T using the current doubly selective DANTE multiple quantum filtering technique, the metabolite null method was used to measure the contribution of macromolecules to the signal intensity at 3.0 ppm in seven of the nine in vivo studies. Using Eq. [1] the macromolecule contribution was calculated to be (12 ± 8)% (mean ± SD, N = 7) of the total signal intensity obtained without the metabolite null. Previous measurements using a standard J-editing sequence at 2.1 T found a 40% contribution in the resultant peak at 3.0 ppm from macromolecules in a similar brain region (8). Therefore, the current doubly selective DANTE multiple quantum method represents a significant improvement in suppression of macromolecule contamination.

In Vivo GABA Quantitation

The intensity of pure GABA can be calculated using the following equation:

$$S_{GABA} = S_{no\ metabilite-null}(1 - f_{macromolecules}). \quad [2]$$

Individual macromolecule fractions were used to calculate GABA intensity for each study except for the two studies that did not use the metabolite null method and $f_{macromolecules}$ = 12% was assumed instead. After subtracting the macromolecule contribution from the measured signal intensity at 3.0 ppm, the concentration of GABA (free GABA + homocarnosine) (28) in the occipital lobe of healthy adult subjects can be quantitated using creatine as an internal standard. To cancel the error introduced by the difference between the STEAM sequence for creatine measurement and the multiple quantum filtering sequence for GABA measurement, including the error due to a mismatch of the excitation profiles generated by the two sequences, the GABA-to-creatine ratio was calibrated on a phantom sample containing GABA and creatine in a 1:8 molar ratio. The same sequences were used to acquire fully relaxed GABA and creatine spectra from the phantom sample. The creatine concentration in the 3 × 3 × 3 cm^3 volume selected in the occipital lobe was assumed to be

7.1 μmol/mL, corresponding to an equal mixture of gray and white matter (10). Using this procedure the concentration of GABA (free GABA + homocarnosine) in the occipital lobe was determined to be 1.21 ± 0.28 μmol/mL, (mean ± SD, $N = 9$).

DISCUSSION

Doubly selective DANTE pulses have previously been used as a refocusing pulse in in vivo lactate editing by alternating the direction of the linear phase increment of the even-numbered RF components (20) and as a doubly selective excitation pulse in high-resolution NMR spectroscopy (21). In this application, the DANTE pulse was used as a doubly selective refocusing pulse to selectively prepare GABA-3 and GABA-4 into a multiple quantum state. As in Ref. 20, the phase increment was set to 90° for the convenience of implementation. Therefore, the interpulse interval is determined by the frequency separation between GABA-3 and GABA-4 resonances at a specific field strength. The only variable for the doubly selective DANTE pulse is its duration or the total number of RF components, i.e., the selectivity of the doubly selective DANTE pulse. As shown in Fig. 2, the first upfield 2π null of the doubly selective DANTE pulse approximately coincides with the frequency offset of the macromolecules at 1.72 ppm, when the total number of RF components is set to 31. The resultant flip angle for each RF component is 11.25° for GABA-4, and 12° for GABA-3, respectively. However, a 90° phase increment is not necessary for spectrometers capable of arbitrary phase shifts, allowing some flexibility in designing the doubly selective DANTE pulse.

The conventional spectrally nonselective 180° refocusing pulse in multiple quantum preparation is replaced here by a doubly selective DANTE π refocusing pulse, with the first set of refocusing bands centered on GABA-3 and GABA-4, respectively. Ignoring the J-evolution and coherence transfer effects during the relatively long DANTE pulse, the evolution of GABA spins under the pulse scheme shown in Fig. 1 is similar to that using a nonselective 180° refocusing pulse in multiple quantum preparation except that here GABA-2 is not refocused by the doubly selective DANTE pulse. Under the approximation of weakly coupled spins, the GABA-3/-4 spin system is prepared by this new method into double quantum coherence DQC_y. In comparison, a nonselective π refocusing pulse prepares the GABA-3/-4 spin system into a mixture of double and zero quantum coherences $(3DQC_y - ZQC_y)/4$ due to the evolution of the GABA-2/-3 J couplings during the multiple quantum preparation period (15). Due to the suppression of zero quantum coherence the yield of the double quantum preparation is theoretically 100% for the two outer lines, compared to a 75% yield using a nonselective preparation (15). This was confirmed using a density matrix simulation assuming weakly coupled spins while taking into account the evolution of the J couplings during the doubly selective DANTE pulse (data not shown).

However, due to the relatively long pulse duration (38.9 ms) and large flip angle (11.25° and 12°) for each RF segment of the doubly selective DANTE pulse, which may lead to significant coherence leakage, the convergence of coherences to GABA-3/-4 antiphase magnetization prior to the second 90° pulse is not intuitively apparent. The results shown in Fig. 3 demonstrate excellent convergence to the GABA-3/-4 antiphase coherence before its conversion to the double quantum spin state using the current doubly selective DANTE pulse as a refocusing pulse for double quantum preparation. In Fig. 3, the experimentally measured GABA retention ratio between the two different methods is somewhat lower than the theoretical prediction of 133%. This is probably due to the lower field strength of 2.1 T used in this study, at which the GABA spins significantly deviate from the weak coupling limit, especially the GABA-2/-3 spins. At 2.1 T the chemical shift-to-J coupling constant ratio is 13.5 for GABA-3/-4 and 4.5 for GABA-2/-3, respectively, indicating strong coupling. The relatively narrow refocusing bandwidth of the DANTE pulse may also have contributed to the signal loss.

The OVS-ISIS localization method was used here to select a $3 \times 3 \times 3$ cm^3 volume. Other methods of localization could also be used. There are two major advantages of the ISIS localization method used here for multiple quantum GABA editing. The first advantage is that it allows GABA measurement from off-centered voxels by simply shifting the frequency of the localization pulses. In comparison, combining spatial localization with multiple quantum preparation can lead to a phase shift of the transverse GABA-3/-4 magnetization, depending on the spatial localization of the selected voxel. The second advantage is that the spin of the overlapping noncoupled creatine resonance at 3.0 ppm is returned to the z axis by the second $90°_x$ pulse (Fig. 1), assuming exact flip angles and perfect RF field homogeneity. Residual transverse terms of the creatine signal due to RF imperfection remain at single quantum state. This allows excellent creatine suppression using a subsequent double quantum filter with relatively weak gradient strength.

As a result, excellent creatine suppression was achieved using both the nonselective and the doubly selective multiple quantum methods. The major disadvantage of the J-editing-based GABA methods is potential errors in creatine subtraction caused by both subject movement and the transient Bloch-Siegert effect (27). Because of the transient Bloch-Siegert effect, the presence of the weak editing pulse on the GABA-3 resonance at 1.91 ppm affects the free precession of the creatine magnetization at 3.0 ppm. The net deviation of creatine from free precession, which can be predicted by rotation matrix calculations, is a nonfactorizable function of the shape, duration, and frequency offset of the editing pulse. This deviation always leads to subtraction errors during J-editing, except for some special circumstances (29) or in cases in which they are compensated for in postacquisition processing (8). Because the creatine signal at 3.0 ppm is ca. 20-fold stronger than the edited GABA-4 signal, slight rotation of the creatine at 3.0 ppm caused by the editing pulse at 1.91 ppm can lead to significant subtraction errors. Multiple quantum-based GABA editing methods, such as the one proposed here, effectively overcome these difficulties with excellent creatine suppression achieved in each single scan. This is because the crucial double quantum filtering gradients are placed immediately before data acquisition. Any RF events after the double quantum filtering gradients could

result in spurious refocused single quantum coherences and significantly compromise creatine suppression. A higher creatine suppression ratio could also be achievable with a gradient strength greater than 1.4×10^{-2} T/m available on the 2.1 T spectrometer.

A variety of cerebral glutathione concentration estimates have been reported in the literature (18). Using nonselective multiple quantum preparation methods, glutathione can be suppressed in the double- to single-quantum conversion step using a selective or semiselective 90° pulse on GABA-3 to selectively convert the GABA-3/-4 double quantum into antiphase single quantum coherence. Using the current method the glutathione cysteinyl methylene group at 2.87–2.94 ppm has only one coupled resonance refocused or partially refocused by the doubly selective DANTE pulse. The effect of selective refocusing of one of the coupled spins is as if the spins were not coupled. Therefore, glutathione is suppressed in a fashion similar to that of creatine. The advantage of the current doubly selective multiple quantum preparation method over the nonselective or semiselective methods is that the suppression of glutathione is achieved using gradient filtering, which is more effective than RF selectivity alone. On the other hand, the method proposed here should be easily adapted for selective measurement of other J-coupled metabolites such as glutathione (18), lactate (29,30), β-hydroxybutyrate (29,31), and glutamate/glutamine.

Excellent macromolecule suppression was also achieved using the current doubly selective multiple quantum GABA editing method. The contribution of macromolecules to the uncorrected signal at 3.0 ppm was measured to be (12 ± 8)% (mean ± SD, $N = 7$) of the total signal intensity. Complete suppression in a single shot of macromolecules at 3.0 ppm is difficult due to a mere 17-Hz separation at 2.1 T between the GABA-3 at 1.91 ppm and the macromolecules at 1.72 ppm, to which the macromolecules at 3.0 ppm are coupled (25). The situation is further complicated by static field inhomogeneity as well as the spread of both the GABA-3 multiplet at 1.91 ppm and the macromolecule multiplets at 1.72 ppm. Experimentally, the macromolecule suppression achieved using the doubly selective multiple quantum method compares favorably with the 40% contribution reported for the J-editing-based GABA method at the same field strength (8). The duration of the doubly selective DANTE pulse was chosen to shift its first upfield 2π null close to the resonant frequency of the macromolecules at 1.72 ppm. At 2.1 T this was achieved by setting the overall length of the doubly selective DANTE pulse to be ca. 45% longer than the singly selective DANTE pulse used for J-editing-based GABA measurement (8). It should be noted that the 2π null scheme used for macromolecule suppression is not specific to the proposed doubly selective multiple quantum filtering method. It could be applied to other GABA editing methods as well. In particular, the macromolecule suppression efficiency of the two-step J-editing-based GABA methods could be improved using the same principle and/or pulse shaping (10). The combination of higher field strength and pulse shaping may hold the key for complete macromolecule suppression in a single shot.

It should also be noted that the IR delay for a metabolite null optimized using the STEAM localization sequence is slightly different from that of the GABA sequence using 3D ISIS localization. This is due to the presence of the hyperbolic secant inversion pulses interfering with the T_1 recovery of the metabolites. This effect is minimized here by placing the three ISIS pulses immediately before the multiple quantum preparation pulses. Nevertheless, the ISIS pulse permutations can be approximated as an alternated single inversion pulse (25). Using the estimated metabolite T_1 of 1.2 s (= 0.86 s/ln2), the uncertainty in GABA contribution to the residual macromolecule signal due to the ISIS inversion in Fig. 5d was estimated to be ~1.3% of the intensity of GABA. Therefore, its effect on GABA quantitation can be safely ignored.

To minimize differential intensity reduction caused by the T_1 relaxation effects, the STEAM sequence for creatine measurement and the ISIS sequence for GABA measurement were matched in TR. In phantom measurements the TR was set to a fully relaxed condition for both sequences. A TR of 3.3 s was used for in vivo measurement of both creatine and GABA. Since the metabolite T_1 was estimated to be 1.2 s the T_1 saturation factor for metabolites is calculated to be approximately 7% for both sequences. Assuming that the difference in T_1 between creatine and GABA is not large at 2.1 T, the differential intensity reduction caused by the T_1 relaxation effects should be negligible.

The effective TE with regard to T_2 relaxation (32) for GABA-3/-4 spins for the doubly selective multiple quantum method can be determined numerically by taking into account of the complicated trajectory of the GABA-3/-4 spins during the doubly selective DANTE pulse. Due to the complexity caused by simultaneous J evolution and the preceding gradient crushers, determination of the effective TE with regard to T_2 relaxation was not pursued. However, the upper limit of the error in GABA quantitation due to the mismatch of the TE of the multiple quantum sequence and that of the STEAM sequence was estimated to be ca. 5%, assuming that all GABA-3/-4 spins are on the transverse plane during the doubly selective DANTE pulse.

Using the doubly selective multiple quantum GABA editing method, we measured an in vivo GABA-to-creatine ratio of 0.17 ± 0.04 (mean ± SD, $N = 9$) after correction of macromolecule contributions. This result is slightly larger than the previous reported GABA-to-creatine ratios of 0.14–0.16 (7,8,10) using J-editing methods with macromolecule corrections. A detailed comparison with the ratios obtained by other methods depends upon using the same spectral quantitation procedures (e.g., integral bandwidth or spectral fitting input functions, apodization, etc.), which is beyond the scope of this work. The 23% relative standard deviation (SD) or coefficient of variance (CV) of the GABA concentration measured in this study is close to the high end of the reported CV range of 9–26% obtained using the J-editing measurements (7,8,10). Under ideal conditions the acquired spectra using the doubly selective multiple quantum GABA editing method should contain no signals other than the one at 3.0 ppm. Due to the imperfect spectral selectivity of the rectangular doubly selective DANTE pulse (Fig. 2) and the low field strength of 2.1 T, other J-coupled metabolites with high concentration (such as glutamate) could also have contributed to the filtered spectra. These residual metabolites should be sup-

pressed in Fig. 5d due to the relative uniformity of the T_1 values of the different metabolites at 2.1 T. Most likely, susceptibility-shifted lipid and/or water signals, which were not completely dephased by the weak gradients available on the 2.1 T system, are the main contributors to the spurious signals at resonances other than 3.0 ppm, as shown in Fig. 5c and d. Such susceptibility-shifted signals could also contribute to the observed signal at 3.0 ppm, therefore causing errors and scattering in the in vivo GABA data. Variations in subjects' sex and age, as well as in the placement of the voxel, may also have contributed to the scattering of the measured GABA concentration.

The measured GABA concentration depends on the assumption of the concentration of the creatine internal standard. In the current study, the center of the voxel was placed in the occipital lobe and 3 cm deep from the dura. Assuming an equal mixture of gray and white matter, which corresponds to a creatine concentration of 7.1 μmol/mL (10), the concentration of GABA (primarily the sum of GABA and homocarnosine (28)) in the selected voxel was determined to be 1.21 ± 0.28 μmol/mL. This measurement could also be complicated by the fact that the creatine signal at TE = 68 ms is contaminated by macromolecules, GABA, and possibly glutathione. However, it should be noted that the same problem exists for all GABA measurements using creatine as an internal standard.

Finally, the method proposed here uses more RF pulses than the J-editing methods. This makes it more susceptible to RF inhomogeneity for a certain RF coil system. Here this problem is minimized by the use of a homogeneous coil for RF transmission. The doubly selective multiple quantum method also uses a 2π null for macromolecule suppression. It therefore requires excellent static field homogeneity within the selected volume for suppression of the overlapping macromolecule signals. This makes it very difficult, if not impossible, to apply it directly to chemical shift imaging of GABA over an extended brain region due to possible significant inhomogeneity in the amplitude of static field. However, recent advances (33, 34) in shimming have substantially improved the volumes in the human brain over which static field homogeneity sufficient for good sequence performance may be obtained, and we have previously demonstrated GABA chemical shift imaging with a multiple quantum coherence selection-based sequence (15). The conversion of the GABA J-editing methods to the chemical shift imaging mode has similar difficulties because the degree of excitation of macromolecules, which strongly depends on the amplitude and frequency offset of the editing pulse, is needed to be uniform across the brain slice to calculate GABA concentration for each individual pixel.

In conclusion, we have demonstrated that by using a doubly selective DANTE refocusing pulse to prepare GABA-3 and GABA-4 into a multiple quantum state, overlapping metabolites and macromolecules can be suppressed in each single scan. Complete suppression of metabolites and significant improvement in suppression of overlapping macromolecules at 3.0 ppm was achieved at the relatively low field strength of 2.1 T. At a higher field strength this method has the potential for single-shot GABA measurement in the brain, with further improvement in the suppression of contaminating macromolecules.

ACKNOWLEDGMENTS

The authors thank Drs. Hoby Hetherington, Jullie Pan, Kevin Behar, Jeff Duyn, Ralph Hurd, and Napapon Sailasuta for helpful discussions; Mr. Terry Nixon for upgrades and support of the spectrometer; and the reviewers for useful suggestions. This work is supported in part by NIH grants R01 RR 15106 (to J.S.) and NS 37527 (to D.L.R.), and a NARSAD Young Investigator Award (to J.S.).

REFERENCES

1. McCormick DA. GABA as an inhibitory neurotransmitter in human cerebral cortex. J Neurophysiol 1989;62:1018–1027.
2. Petroff OAC, Rothman DL, Behar KL, Mattson RH. Initial observation on effect of vigabatrin on *in vivo* ^{1}H spectroscopic measurement of γ-aminobutyric acid, glutamate, and glutamine in human brain. Epilepsia 1995;36:457–464.
3. Petroff OAC, Behar KL, Mattson RH, Rothman DL. Human brain γ-aminobutyric acid levels and seizure control following initiation of vigabatrin therapy. J Neurochem 1996;67:2399–2404.
4. Petroff OAC, Rothman DL, Behar KL, Collins TL, Mattson RH. Human brain GABA levels rise rapidly after initiation of vigabatrin therapy. Neurology 1996;47:1567–1571.
5. Sherif FM, Ahmed SS. Basic aspects of GABA-transaminase in neuropsychiatric disorders. Clin Biochem 1995;28:145–154.
6. Behar KL, Rothman DL, Petersen KF, Hooten M, Deleney R, Petroff OAC, Shulman GI, Navarro V, Petrakis IL, Charney DS, Krystal JH. Preliminary evidence of low cortical GABA levels in localized ^{1}H-MR spectra of alcohol-dependent and hepatic encephalopathy patients. Am J Psychiatry 1999;156:952–954.
7. Sanacora G, Mason GF, Rothman DL, Behar KL, Hyder F, Petroff OAC, Berman RM, Charney DS, Krystal JH. Reduced cortical γ-aminobutyric acid levels in depressed patients determined by proton magnetic resonance spectroscopy. Arch Gen Psychiatry 1999;56:1043–1047.
8. Rothman DL, Petroff OAC, Behar KL, Mattson RH. Localized ^{1}H NMR measurement of γ-aminobutyric acid in human brain *in vivo*. Proc Natl Acad Sci USA 1993;90:5662–5666.
9. Keltner JR, Wald LL, Christensen JD, Maas LC, Moore CM, Cohen BM, Renshaw P. A technique for detecting GABA in the human brain with PRESS localization and optimized refocusing spectral editing radiofrequency pulses. Magn Reson Med 1996;36:458–461.
10. Hetherington HP, Newcomer BR, Pan JW. Measurement of human cerebral GABA at 4.1 T using numerically optimized editing pulses. Magn Reson Med 1998;39:6–10.
11. Mescher M, Merkle H, Kirsch J, Garwood M, Gruetter R. Simultaneous *in vivo* spectra editing and water suppression. NMR Biomed 1998;11:266–272.
12. Ke Y, Cohen BM, Bang JY, Yang M, Renshaw PF. Assessment of GABA concentration in human brain using two-dimensional proton magnetic resonance spectroscopy. Psychiatr Res 2000;100:169–178.
13. de Graaf RA, Santovito M, Duyn JH, Rothman DL. GABA detection by longitudinal scalar order difference editing. In: Proceedings of the 8th Annual Meeting of ISMRM, Denver, 2000. p 605.
14. Keltner JR, Wald LL, Frederick B, Renshaw P. *In vivo* detection of GABA in human brain using a localized double-quantum filter technique. Magn Reson Med 1997;37:366–371.
15. Shen J, Shungu DC, Rothman DL. *In vivo* chemical shift imaging of γ-aminobutyric acid in the human brain. Magn Reson Med 1999;41:35–42.
16. Henry P-G, Dautry C, Hantraye P, Bloch G. Brain GABA editing without macromolecule contamination. Magn Reson Med 2001;45:517–520.
17. Cooper AJL. Role of astrocytes in maintaining cerebral glutathione homeostasis and in protecting the brain against xenobiotics and oxidative stress. In: Shaw CA, editor. Glutathione in the nervous system. London: Taylor & Francis; 1998. p 91–115.

18. Trabesinger AH, Weber OM, Duc CO, Boesiger P. Detection of glutathione in the human brain *in vivo* by means of double quantum coherence filtering. Magn Reson Med 1999;42:283–289.
19. Morris GA, Freeman R. Selective excitation in Fourier transform nuclear magnetic resonance. J Magn Reson 1978;29:433–462.
20. Blondet P, Albrand P, von Kienlin M, Decorps M, Lavanchy N. Use of rotating-phase DANTE pulses for *in vivo* proton NMR spectral editing with a single irradiation facility. J Magn Reson 1987;71:342–346.
21. Geen H, Wu X-L, Xu P, Friedrich J, Freeman R. Selective excitation at two arbitrary frequencies. The double-DANTE sequence. J Magn Reson 1989;81:646–652.
22. Gruetter R. Automatic localized *in vivo* adjustment of all first- and second-order shim coils. Magn Reson Med 1993;29:804–811.
23. Shen J, Rycyna RE, Rothman DL. Improvements on an *in vivo* automatic shimming method (FASTERMAP). Magn Reson Med 1997;38:834–839.
24. Kupce E, Freeman R. Close encounters between soft pulses. J Magn Reson A 1995;112:261–264.
25. Behar KL, Rothman DL, Spencer DD, Petroff OAC. Analysis of macromolecule resonances in ^{1}H NMR spectra of human brain. Magn Reson Med 1994;32:294–302.
26. Blumich B, Spiess HW. Quaternions as a practical tool for the evaluation of composite pulses. J Magn Reson 1985;61:356–362.
27. Emsley L, Bodenhausen G. Optimization of shaped selective pulses for NMR using a quaternion description of their overall propagators. J Magn Reson 1992;97:135–148.
28. Rothman DL, Behar KL, Prichard JW, Petroff OAC. Homocarnosine and the measurement of neuronal pH in patients with epilepsy. Magn Reson Med 1997;32:924–929.
29. Shen J, Novotny EJ, Rothman DL. *In vivo* lactate and β-hydroxybutyrate editing using a pure phase refocusing pulse train. Magn Reson Med 1998;40:783–788.
30. Hurd RE, Freeman DM. Metabolic specific proton magnetic resonance imaging. Proc Natl Acad Sci USA 1989;86:4402–4406.
31. Pan JW, Rothman DL, Behar KL, Stein DT, Hetherington HP. Human brain beta-hydroxybutyrate and lactate increase in fasting-induced ketosis. J Cereb Blood Flow Metab 2000;20:1502–1507.
32. Hajduk PJ, Horita DA, Lerner LE. Theoretical analysis of relaxation during shaped pulses. I. The effects of short T_1 and T_2. J Magn Reson A 1993;103:40–52.
33. Shen J, Rothman DL, Hetherington HP, Pan JW. Linear projection method for automatic slice shimming. Magn Reson Med 1999;42:1082–1088.
34. Shen J. Effect of degenerate spherical harmonics and a method for automatic shimming of oblique slices. NMR Biomed 2001;14:177–183.